JOURNAL OF BACTERIOLOGY, Oct. 1991, p. 6213–6222
0021-9193/91/196213-10$02.00/0

Vol. 173, No. 19

Dissolution and Immunochemical Analysis of the Sheath of the Archaeobacterium *Methanospirillum hungatei* GP1

G. SOUTHAM AND T. J. BEVERIDGE*

Department of Microbiology, College of Biological Science, University of Guelph, Guelph, Ontario N1G 2W1, Canada

Received 18 April 1991/Accepted 19 July 1991

The sheath of *Methanospirillum hungatei* GP1 was degraded by three dissolution techniques, which produced a range of soluble products. By using 0.05 M L-arginine buffer (pH 12.6) at 90°C for 10 min, 74% (dry weight) of the sheath was dissolved; however, the solubilized polypeptides were extensively degraded. Treatment with 2% β-mercaptoethanol and 2% sodium dodecyl sulfate at 90°C in 0.05 M 2(*N*-cyclohexylamino)ethanesulfonic acid (CHES) buffer (pH 9.0) solubilized 42% (dry weight) of the sheath as a group of polypeptides of 30 to 40 kDa. At 100°C for 2 h, 5% β-mercaptoethanol, 2% sodium dodecyl sulfate (SDS), and 20 mM EDTA released 74% of the sheath's mass as a group of polypeptides of 10 to 40 kDa. All solubilized products were examined by SDS-polyacrylamide gel electrophoresis, and a range of high- and low-molecular-weight polypeptides was identified. None were glycoproteins. Hoops, which comprise the sheath's structure, were seen by electron microscopy after all of the attempted dissolutions. Monoclonal antibodies were produced against the 10- to 40-kDa range of solubilized products and against the ~40-kDa polypeptides, and polyclonal antiserum was produced against an 18-kDa polypeptide. These immunological markers were used in Western immunoblotting and protein A-colloidal gold-antibody probing by electron microscopy to identify the structural location of the various polypeptides. Native sheath, which possesses 2.8-nm particles on its outer surface (M. Stewart, T. J. Beveridge, and G. D. Sprott, J. Mol. Biol. 183:509–515, 1985; P. J. Shaw, G. J. Hills, J. A. Henwood, J. E. Harris, and D. B. Archer, J. Bacteriol. 161:750–757, 1985), presented a gentle wave-form surface in platinum-shadowed specimens. In contrast, the inner face of the sheath was highlighted by ridges lying perpendicular to the longitudinal axis of the sheath and likely corresponded to hoop boundaries. Both the polyclonal and monoclonal antibodies were specific for different faces; polyclonal antibodies labeled the inner face, whereas monoclonal antibodies labeled the outer face. Accordingly, the apparent asymmetry of structure between the two faces of the sheath can be correlated by our immunochemical probing with a distinct asymmetry in the distribution of exposed polypeptides between the faces. The possible implications of this asymmetry for growth and maturation of the sheath are explained.

Correlation of the structure and chemistry of bacterial surface arrays (S layers) must ultimately focus on how the constituent tertiary protein subunits assemble into two-dimensional paracrystalline arrays. Previous studies have shown that covalent linkage is not involved in subunit-subunit interactions and that self-assembly is possible. For this reason, solubilized S layers, especially those from gram-positive eubacteria, can be reassembled in vitro by simply removing the solubilizing agent (22). These solubilizing agents typically modify ionic or hydrogen bonding or hydrophilic-hydrophobic interactions.

The proteinaceous sheath of *Methanospirillum hungatei* GP1 is an unusual bacterial S layer. Chemical analysis of the sheath has proven difficult because of its stability in the presence of typical chaotropic and nonionic detergents, denaturants, and digestive enzymes (4). Sprott et al. (23) developed an alkali dissolution technique for the examination of the molecular components of the sheath structure. Their sheath model, developed to correlate these solubilized components to the intact sheath structure, consisted of a 24-kDa surface array protein overlying a high-molecular-mass (>10^3 kDa) inner region. They also described a second dissolution technique which utilized sodium dodecyl sulfate (SDS) and β-mercaptoethanol (β-ME). However, they were unable to separate distinct solubilized sheath components by high-performance liquid chromatography by using this second technique.

Examination of the results of sheath dissolution techniques by SDS-polyacrylamide gel electrophoresis (SDS-PAGE) has had only limited success (6, 23). Our present study suggests that this has been due to the limited efficiency of sheath dissolution, the utilization of extremely harsh dissolution techniques, or a combination of the two. Proper evaluation of the sheath's chemical complexity has required time course studies on dissolution by using transmission electron microscopy (TEM) and, eventually, SDS-PAGE analysis of the solubilized polypeptides. We also employed immunological probes to relate these solubilized polypeptides to the intact sheath structure.

MATERIALS AND METHODS

Bacterial growth conditions. *M. hungatei* GP1 (18) was grown in 20-liter glass carboys, each containing 4 liters of SA medium (17). The culture vessels were maintained at 37°C and pressurized twice daily with H_2 and CO_2 (4:1).

Purification of sheath. A crude preparation of *M. hungatei* sheath was obtained through spheroplast formation in cell cultures (24) and sucrose gradient centrifugation (25). The crude sheath preparation was resuspended in 100 ml of 0.1 M NaOH to remove spacer plugs and gently agitated at room temperature for 1 h. This material was centrifuged at 15,000 × *g* for 45 min. The pellet was washed in 0.1 M NaOH and

* Corresponding author.

then in distilled water (dH_2O) and centrifuged at 15,000 × *g* for 45 min between washes. The final pellet was resuspended in dH_2O to a final volume of 30 ml. The sheath suspension was then layered over 60% (wt/vol) sucrose (Sigma Chemical Co., St. Louis, Mo.) (1 volume of sheath to 6 volumes of sucrose) and centrifuged at 90,000 × *g* for 18 h. The pellet was washed, as before, four times with dH_2O. The sheath preparation was resuspended in 100 ml of 1% (wt/vol) SDS (Bio-Rad Laboratories, Richmond, Calif.), incubated at 90°C for 45 min to remove contaminating cellular debris, and again washed four times with dH_2O. Electron microscopy (EM) of this material showed it to be free of all cellular debris and cell spacers. The final pellet was resuspended in 100 ml of dH_2O containing 0.01% (wt/vol) sodium azide as a preservative and stored at 4°C. The azide was removed from the sheath preparation by washing it by centrifugation (14,000 × *g* for 1 min) prior to further experimentation.

Physical and chemical fractionation of sheath. Purified sheath (5 ml of a 6.6-mg/ml suspension) was passed through a French pressure cell (Aminco) at 124 kPa. The shear forces produced by this treatment fractured the sheath and allowed the examination (by TEM) of single-layer fragments of platinum-shadowed specimens.

Three chemical methods were employed to solubilize *M. hungatei* sheath. The first treatment used the alkali dissolution technique of Sprott et al. (23) and a more extended version of this technique involving the dialysis of sheath (1.2 mg) in 0.05 M L-arginine (L-Arg) (pH 12.6, 200 ml) for 7 days at room temperature. The second treatment, also described by Sprott et al. (23), involved the reaction of sheath with 2% (wt/vol) SDS and 2% (vol/vol) β-ME in 0.05 M 2(*N*-cyclohexylamino)ethanesulfonic acid (CHES) (Sigma) buffer (pH 9.0) (SDS/β-ME/CHES) at 90°C for 30 min. The third treatment, incubation of sheath in SDS-PAGE dissolution buffer (11) for 2 h at 100°C, represented a modification of the second method. The SDS-PAGE dissolution buffer consists of 0.125 M Tris-HCl (pH 6.8) containing 5% β-ME, 2% SDS, and 20 mM EDTA (Sigma) (SDS/β-ME/EDTA). Purification of the 18-kDa protein (solubilized by the SDS/β-ME/EDTA treatment) involved cutting this band from SDS-polyacrylamide gels, elution by diffusion into dH_2O, and concentration by freeze-drying. This preparation was used for the production of polyclonal antisera.

Efficiency of sheath solubilization. In an attempt to determine the solubilization efficiency of these treatments, sheath was reacted separately by using each of the dissolution conditions. These preparations were then centrifuged at 175,000 × *g* for 1 h to separate soluble from insoluble material and were placed in preweighed aluminum planchets (Sigma) and dried at 110°C until the dry weights were stable. These values were compared with those of untreated sheath controls.

Protein determination. Protein concentrations were assayed by the modified Lowry procedure described by Markwell et al. (14). Bovine serum albumin (Sigma) was used as a standard.

SDS-PAGE. Samples from the L-Arg treatment and the SDS/β-ME/CHES treatment were neutralized with 1 M HCl as monitored with Short Range Alkacid pH paper (Fisher Scientific). The samples then received enough glycerin to bring their concentration to 5% (wt/vol) and to facilitate their loading onto a polyacrylamide gel. Purified sheath was also solubilized with SDS/β-ME/EDTA at 100°C for 2 h. A Protean-II Mini-Gel System (Bio-Rad) was routinely used for SDS-PAGE by the method of Laemmli (11). These samples were run in a 15% resolving gel and examined. Gels were routinely stained and fixed with 0.5% Coomassie brilliant blue R250 (Sigma) in 40% methanol–10% acetic acid for 1 h at room temperature. Destaining required multiple changes of 40% methanol–10% acetic acid.

Glycoprotein staining. SDS-polyacrylamide gels containing the solubilized sheath preparations were examined for the presence of glycoproteins by the periodic acid-Schiff staining method described by Fairbanks et al. (7). Bovine A-1 glycoprotein (Sigma) was used as a positive control for glycoprotein staining.

Production of Pαsera. The 18-kDa protein purified from the SDS/β-ME/EDTA dissolution of purified sheath was used to initiate the production of specific polyclonal antisera (Pαsera) in New Zealand White rabbits. Each injection contained 100 μg of protein. The immunization schedule for the rabbit was as follows: days 1 and 4, subcutaneous injections of a 1:1 mixture of antigen and Freund's incomplete adjuvant (Difco, Detroit, Mich.); days 7 and 14, intramuscular injections of the same antigen preparation injected on days 1 and 4; day 28, intravenous injection of antigen containing no adjuvant. On day 31, the animal was bled from the ear vein and approximately 20 ml of blood was collected. The blood was left to clot at room temperature for 30 min and transferred to 37°C for an additional 30 min to further separate the serum from the cells. The serum was collected by centrifugation at 14,000 × *g* for 1 min and stored at −20°C.

Hybridoma production. The immunization schedule for BALB/c mice (female, 8 to 10 weeks old; Charles River Canada Inc., St. Constant, Quebec, Canada) was as follows: a subcutaneous injection (0.1 ml) of pure sheath (100 μg [dry weight]) mixed with Freund's incomplete adjuvant (1:1); on day 10, an intraperitoneal injection with 0.1 ml of the same preparation; on day 14, an intravenous boost of 0.1 ml of sheath (100 μg) containing no adjuvant (injected into the tail vein). The mice were sacrificed on day 18, and their spleens were removed. Hybridomas were produced by the method of Oi and Herzenberg (16), with slight modifications, from the primed spleen cells and NS-1 myeloma cells. The fusogen contained 40% polyethylene glycol (1,300 to 1,600 Da; Sigma) and 4% dimethyl sulfoxide (Sigma) in supplemented Dulbecco modified Eagle medium (DMEM; Flow Laboratories, Mississauga, Ontario, Canada) as described by Lane (13).

Selection of hybridomas. Two weeks postfusion, visible colonies of growing hybridoma clones were transferred from 24-well tissue culture (TC) plates (Linbro; Flow Laboratories) to 96-well TC plates. These colonies were allowed to grow for 24 to 48 h in DMEM containing 20% (vol/vol) fetal bovine serum, 100 μM hypoxanthine (Sigma), and 16 μM thymidine (Sigma). The colony supernatants were assayed by an enzyme-linked immunosorbent assay (ELISA) (15). For this assay, 1.5% gelatin in phosphate-buffered saline (PBS) was used as a blocking agent, 5 μg of sheath per well was used as the antigen, and 100-μl samples of culture supernatants were assayed for activity towards the sheath antigen. Positive binding of the primary antibody was determined with rabbit anti-mouse antibody conjugated to alkaline phosphatase with nitrophenyl phosphate (Sigma) as the enzyme-substrate system. The colorimetric reaction was allowed to proceed for 1 h at 37°C and the A_{405} was read with a Titertek Multiskan Spectrophotometer. Hybridomas secreting antibodies specific for the sheath were expanded in 96-well TC plates and cloned by limiting dilutions.

Briefly, the positive hybridomas were diluted to concentrations of 10 and 20 cells per ml and plated into 96-well TC

plates (200 μl per well) in the presence of 5×10^5 feeder cells per ml (mouse thymocytes). Single clones from the limiting-dilution 96-well TC plates were screened by ELISA as described above. The positive clones resulting from limiting dilutions were recloned by limiting dilutions (described above), and positive clones (determined by ELISA) were expanded to produce hybridoma culture supernatants containing monoclonal antibodies for the immunochemical analysis of *M. hungatei* GP1 sheath. These monoclonal antibodies (MAbs) were confirmed and further characterized with a MouseTyper kit (Bio-Rad). The culture supernatants were stored at −20°C prior to use.

Western immunoblotting. The SDS/β-ME/EDTA-solubilized polypeptides were studied by Western immunoblotting using both Pαsera and MAbs from culture supernatants. Samples resolved by SDS-PAGE were electroblotted onto a nitrocellulose membrane (LKB, Bromma, Sweden) (5, 27), and sites without antigen were blocked with 1% gelatin in PBS (0.01 M phosphate, 0.14 M NaCl). MAbs (1/10 dilution) and Pαsera (1/100 dilution) were used as immunological probes to discern their specificities for sheath components and to identify sheath solubilization products. Binding of MAbs was detected with a goat anti-mouse immunoglobulin G conjugated to alkaline phosphatase (Jackson Immunochemicals Inc., West Grove, Pa.) and a Nitro Blue Tetrazolium–5-bromo-3-chloro-indoylphenyl (NBT/BCIP) substrate system (Sigma) (12). The Pαsera was detected by goat anti-rabbit antibody conjugated to alkaline phosphatase (Jackson Immunochemicals) and the same substrate system. The Protean II Blotting apparatus (Bio-Rad) was routinely used for all electroblotting.

TEM. For negative staining, a Formvar carbon-coated copper 200-mesh grid was floated on the sample, removed, allowed to dry, and then washed extensively with dH_2O. The grid was then touched briefly to a 0.1% (wt/vol) peptone solution as a wetting agent, blotted with Whatman no. 1 filter paper, touched to a drop of 2% (wt/vol) uranyl acetate, blotted again, and allowed to dry. These preparations were examined at 60 kV in a Philips EM300 EM operating under standard conditions with the cold finger in place.

For platinum shadowing for TEM, the specimens were applied to Formvar carbon-coated grids as described for negative stains. The grids were then placed in a Balzer model BA 360M freeze-etcher and shadowed by using a 3-cm platinum wire at an angle of 45°. These grids were then examined with the Philips EM300.

Standard embedding of immunolabeled sheath for thin sectioning involved fixation with 1% (wt/vol) glutaraldehyde (Marivac Ltd., Halifax, Nova Scotia, Canada) in 0.05 M 4-(2-hydroxyethyl)-1-piperazineethanesulfonic acid (HEPES) buffer (Research Organics Inc., Cleveland, Ohio), pH 7.2, overnight at 4°C and enrobement in 2% (wt/vol) Noble agar (Difco). Samples were next treated with 2% (wt/vol) osmium tetroxide at room temperature for 1 h and then with 2% uranyl acetate at room temperature for 1 h. The enrobed samples were then processed through an ethanol-propylene oxide dehydration series, as follows: 25% (vol/vol), 50% (vol/vol), 80% (vol/vol), 95% (vol/vol), and 100% ethanol changes; ethanol-propylene oxide (1:1) through two changes; 100% propylene oxide (twice); and finally suspension in propylene oxide-Epon 812 (Can-em, Guelph, Ontario, Canada) (1:1) overnight at room temperature and embedding in Epon 812. Blocks were cured at 60°C for 48 h. Sections (ca. 70 nm thick; Reichert-Jung Ultramicrotome model OMU2) were collected on Formvar carbon-coated grids, poststained with 2% uranyl acetate (7 min) and 2% (wt/vol) lead citrate (10 min), and examined by TEM.

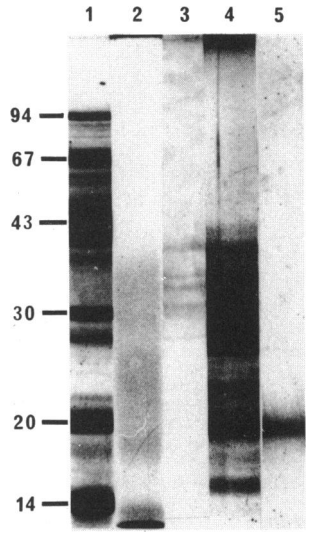

FIG. 1. Coomassie brilliant blue R250-stained SDS–15% polyacrylamide gel of the various sheath dissolution conditions used in this study. Lanes: 1, Bio-Rad low-molecular-weight standards; 2, L-Arg-solubilized sheath at pH 12.6 and 90°C for 10 min; 3, SDS/β-ME/CHES (pH 9.0) treatment at 90°C for 30 min; 4, sheath treated with SDS/β-ME/EDTA for 2 h at 100°C; 5, 18-kDa purification product treated with SDS/β-ME/EDTA (pH 6.8) for 5 min at 100°C. L-Arg (lane 2) did not solubilize discrete proteins and is considered to be a harsh dissolution procedure. Note the large quantity of material at the dye front. The efficiency of sheath solubilization with SDS/β-ME/CHES treatment (lane 3) was low compared with what was observed with SDS/β-ME/EDTA treatment (lane 4). The 18-kDa protein preparation (lane 5) demonstrates the purity of the antigen used to induce the rabbit anti-18-kDa Pαsera. Lanes 2, 3, and 4 received ~60 μg of starting sheath material (following the procedure of Sprott et al. [23]) prior to solubilization, while lane 5 received ~5 μg of protein. Molecular masses are in kilodaltons.

Colloidal gold labeling. Approximately 400 μg of sheath was resuspended either in 0.5 ml of culture supernatant from the growth of MAb-producing cell lines or in 50 μl of Pαsera diluted in 0.45 ml of PBS containing 0.1% (vol/vol) Tween 20 (Sigma), 0.1% (wt/vol) bovine serum albumin (Sigma), and 0.1% (wt/vol) sodium azide (PBS/TBA). This reaction mixture was allowed to incubate at room temperature for 2 h. It was then washed in PBS/TBA by centrifugation for 1 min at 14,000 × *g*, and the resulting pellet was resuspended into 200 μl of PBS/TBA containing 60 μl of protein A (Boehringer Mannheim, Dorval, Quebec, Canada)-colloidal gold (produced by the method of Frens [8] with modifications by Bendayan [1] and Hicks and Molday [9]). This mixture was again incubated for 2 h at room temperature and washed as before. A sample was removed for the examination of whole mounts (with or without negative staining) by TEM to ascertain the distribution pattern of the antibody-protein A-colloidal gold complexes. The remaining material was processed by standard Epon 812 embedding for thin sectioning to ascertain inner or outer surface localization on the sheath.

RESULTS

Comparison of dissolution techniques by SDS-PAGE and TEM. A Coomassie brilliant blue R250-stained SDS-PAGE

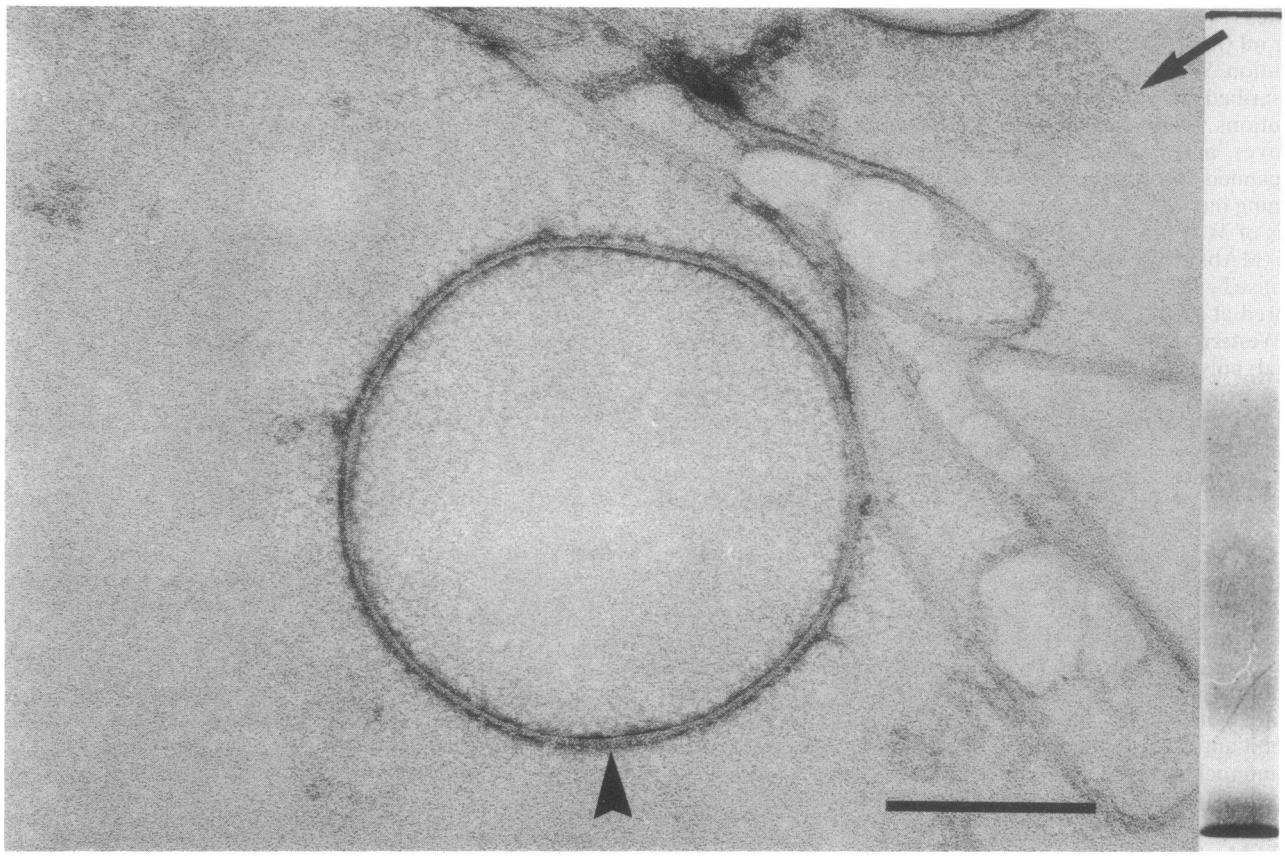

FIG. 2. Negative stain (using 2% [wt/vol] uranyl acetate) of *M. hungatei* GP1 sheath treated with 0.05 M L-Arg (pH 12.6) at 100°C for 10 min. Note the faint 2.8-nm striations on the outer surface of the hoops (arrowhead). Also note that this particulate material does not enter a 15% resolving gel (right). Bar, 0.2 μm. The arrow points from the band in the resolving gel to the particulate material as seen by electron microscopy.

profile of solubilized sheath polypeptides is shown in Fig. 1. Examination of sheath treated with 0.05 M L-Arg, pH 12.6, for 10 min at 90°C demonstrated a broad, poorly stained, uneven range of proteinaceous material which extended throughout the resolving gel, although regions of more intense staining were evident (Fig. 1, lane 2). This suggested that L-Arg sheath solubilization was an excessively harsh process which indiscriminately broke up the sheath constituents and, presumably, affected covalent bonds. Several polypeptides were evident in the SDS/β-ME/CHES extract, but they were in low amounts (Fig. 1, lane 3). This dissolution technique was described by Sprott et al. (23) as an effective method for sheath solubilization. Examination of the SDS/β-ME/EDTA dissolution procedure by SDS-PAGE (Fig. 1, lane 4) revealed a new polypeptide banding pattern. The polypeptides ranged from 10 to 40 kDa, as opposed to the 30- to 40-kDa region evident from SDS/β-ME/CHES-solubilized sheath (Fig. 1; cf. lanes 3 and 4). The SDS/β-ME/EDTA-solubilized proteins were also present in a much higher concentration than those after the SDS/β-ME/CHES solubilization. Very faint periodic acid-Schiff staining was observed only with the insoluble hoops (trapped in the stacking gel) remaining after SDS/β-ME/EDTA sheath dissolution (data not shown).

Treatment of *M. hungatei* GP1 sheath with 0.05 M L-Arg, pH 12.6, at 90°C for 10 min was successful in breaking the intact sheath tubes. Examination by EM of negatively stained material from this preparation demonstrated the presence of small numbers of intact hoops possessing faint 2.8-nm striations on their external surfaces (Fig. 2). The efficiency after 10 min of this solubilization procedure was 74% as determined by the mass of sheath material released.

The SDS/β-ME/CHES and the SDS/β-ME/EDTA dissolution procedures also did not completely solubilize the sheath, releasing 42 and 74% of the sheath's mass, respectively. The insoluble fractions (corresponding to 58 and 26% of the sheath's mass, respectively) contained hoops possessing well-defined 2.8-nm striations on the hoop's outer surface (Fig. 3). Even TEM examination of sheath treated with SDS/β-ME/EDTA for 48 h at 100°C revealed the presence of some hoops, demonstrating the remarkable resiliency of the hoop structure (data not shown). At this point, it is impossible for us to determine which of the low-molecular-weight products derived after each of the chemical treatments are intact monomeric subunits and which are breakdown products.

Structural characterization of the two faces of the sheath. The sheath of *M. hungatei* has been characterized by its remarkable paracrystalline structure when viewed by high-resolution negative stains (4, 26) (Fig. 4). Platinum shadowing is not very highly resolving but is best for overall topography by TEM (3); it revealed that the outer face of the sheath possesses a gentle wave pattern (Fig. 5) which corresponds to the hoops (Fig. 2 and 3). There is no evidence

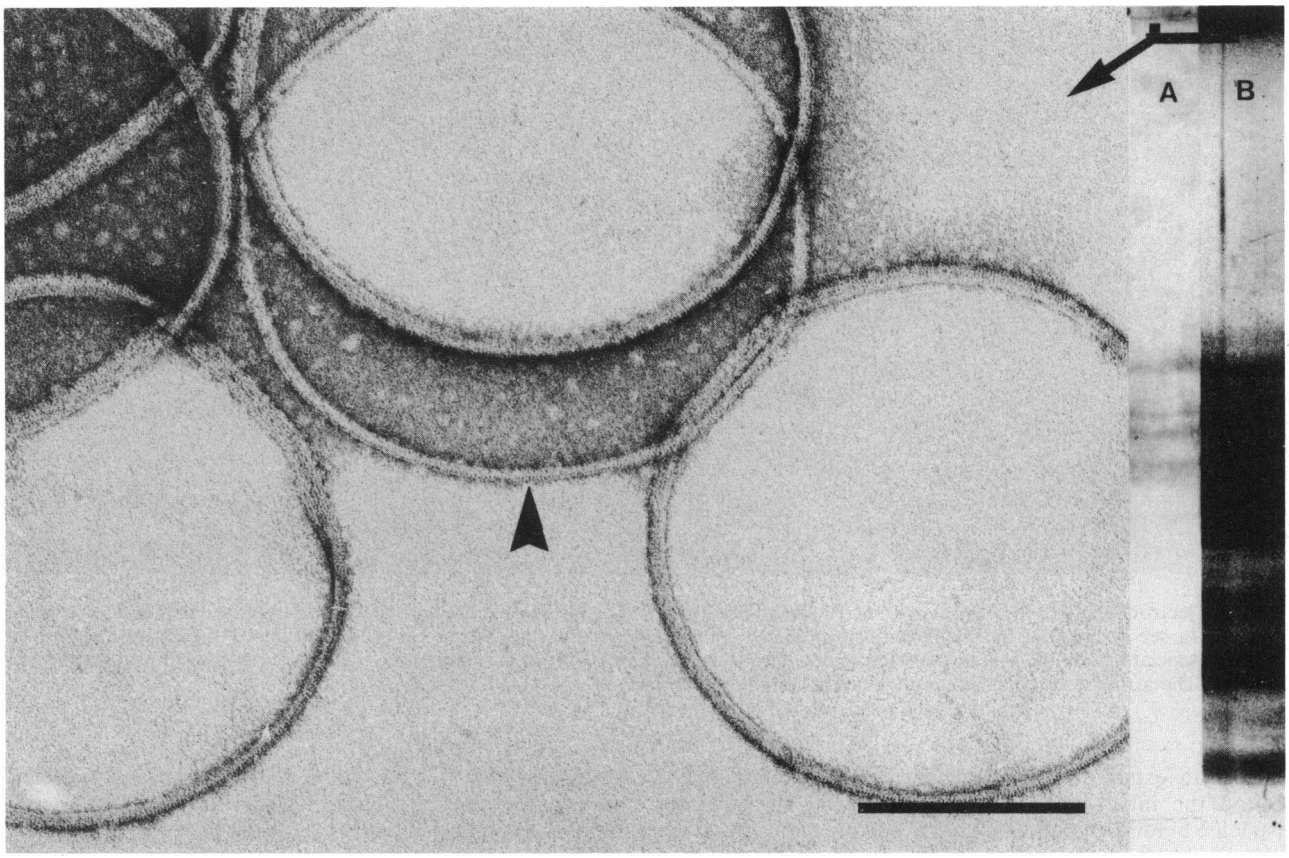

FIG. 3. Negative stain of sheath treated with SDS/β-ME/CHES (pH 9.0) at 90°C for 30 min. Few proteins were solubilized from the sheath by using this treatment (A). Note the 2.8-nm repeat, which is still intact after this sheath dissolution procedure (arrowhead). The SDS/β-ME/EDTA sheath treatment also resulted in the production of similar hoops (data not shown); however, a greater quantity of the sheath was solubilized (B). Bar, 0.2 μm. The arrow points from the band in the resolving gel to the particulate material as seen by electron microscopy.

of the 2.8-nm repeat on the surface of the sheath by this technique, which is not surprising since the platinum grain approaches protein subunit size and cannot penetrate between particles. Examination of sheared sheath which had been shadowed with platinum revealed a remarkable structural difference between the inner and outer surfaces of the sheath (Fig. 6). Interestingly, the inner sheath region possesses ridges lying perpendicular to the longitudinal axis of the sheath. These ridges did not exceed 2.0 nm in height above the general plane of the inner surface (as determined by the length of the shadows cast). These ridges likely represent boundaries between sheath hoops when the scalloped edges of sheath thin-section profiles are taken into account (data not shown).

Immunolabeling. Because of their exquisite specificity, MAbs were selected for use in the characterization of *M. hungatei* GP1 sheath. Two fusions resulted in the production of 304 clones which were screened by ELISA, using 5 μg of purified sheath as antigen. The ELISA demonstrated that 69 of the 304 hybridomas were secreting antibody specific to the sheath of *M. hungatei* GP1. After cloning and recloning by limiting dilutions, two hybridoma clones, specific to the SDS/β-ME/EDTA-solubilized polypeptides, were selected for use as immunological probes.

The chemical resiliency of the sheath (4) makes it a rather unique biological structure to immunoprobe; clearly, for Western immunoblot analysis, a structure must be capable of solubilization and must have a consistent solubilization pattern. While the L-Arg treatment solubilized 74% of the sheath's dry mass, the soluble components varied considerably in molecular weight, and no definite protein bands were observed by SDS-PAGE analysis (Fig. 1, lane 2). Therefore, this technique was considered too harsh for the chemical characterization of the sheath, and its study was discontinued. The SDS/β-ME/CHES dissolution technique was capable of releasing several polypeptides; however, even after extended incubation, only 42% solubilization, as determined by mass analysis, was achieved. Because of this low sheath dissolution efficiency, this technique was also discontinued.

The SDS/β-ME/EDTA-solubilized sheath fraction was selected as the best example of solubilized sheath for Western immunoblot analysis. Two types of immunological probes against the SDS/β-ME/EDTA-solubilized polypeptides were noted. First, immunochemical specificity towards the entire range of the solubilized proteins was observed for MAb 25.1 (Fig. 7, lane 3; the epitope must be preserved on all the 10- to 40-kDa polypeptides) and the rabbit anti-18-kDa Pαsera (Fig. 7, lane 5), whereas a more defined conformation was required for the reactivity of MAb 26.1 (Fig. 7, lane 4).

Now that immunoblotting had established the reactivity of MAb 25.1, MAb 26.1, and rabbit anti-18-kDa Pαsera, it was

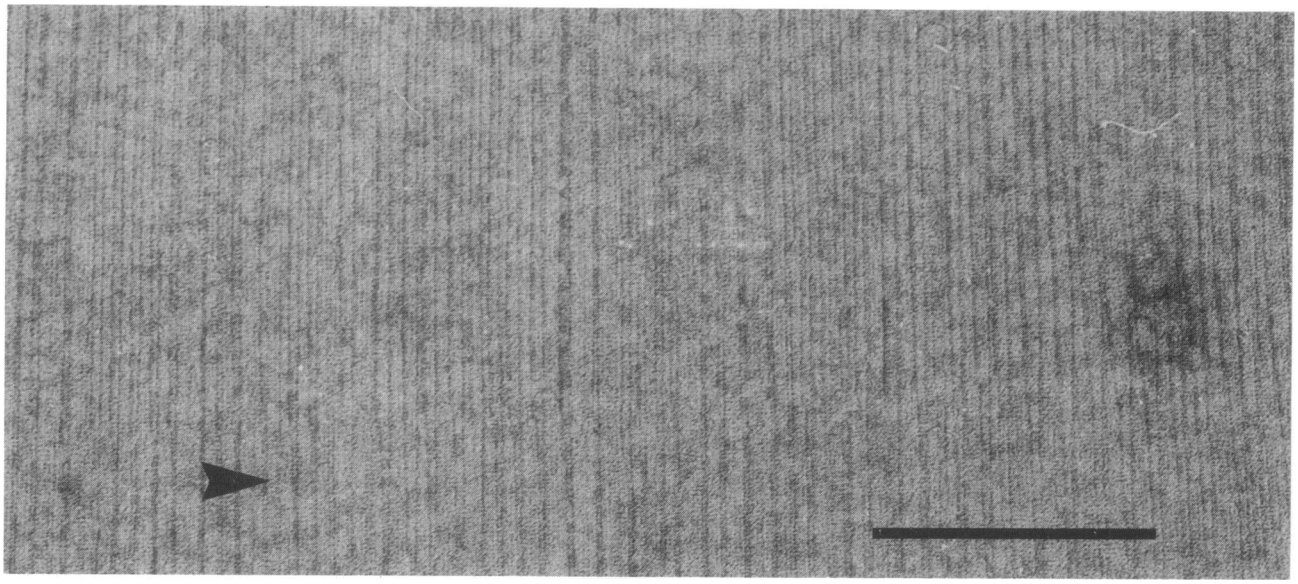

FIG. 4. Electron micrograph of *M. hungatei* GP1 sheath negatively stained with 2% uranyl acetate. Hoop (refer to Fig. 2 and 3) boundaries are difficult to see because of the moiré pattern produced by imaging through the two layers of the collapsed sheath tube. The 2.8-nm periodicity associated with the sheath's surface is most easily seen by holding the micrograph parallel to the eye and looking along the length of the tube. The arrowhead indicates the longitudinal orientation of the sheath. Bar, 0.2 μm.

important to establish exactly where these antibodies reacted on the intact sheath. Control experiments for the nonspecific binding of colloidal gold involving antibody with colloidal gold alone (data not shown) or protein A-colloidal gold (Fig. 8) were all negative.

Sites of attachment of MAb 25.1, MAb 26.1, and rabbit anti-18-kDa Pαsera were visualized by using protein A-colloidal gold and were shown on whole mounts to be randomly distributed over the sheath (Fig. 9 is representative). Examination of thin sections of these preparations revealed a remarkable labeling pattern. MAbs 25.1 and 26.1, which represent a broad chemical and a more restricted (possibly conformational) antibody probe, respectively, were localized exclusively on the external face of the sheath (Fig. 10). However, the rabbit anti-18-kDa Pαsera, an immunological probe also possessing broad chemical specificity, bound protein A-colloidal gold predominantly on the inner face of the sheath (Fig. 11). The assignment of chemical versus

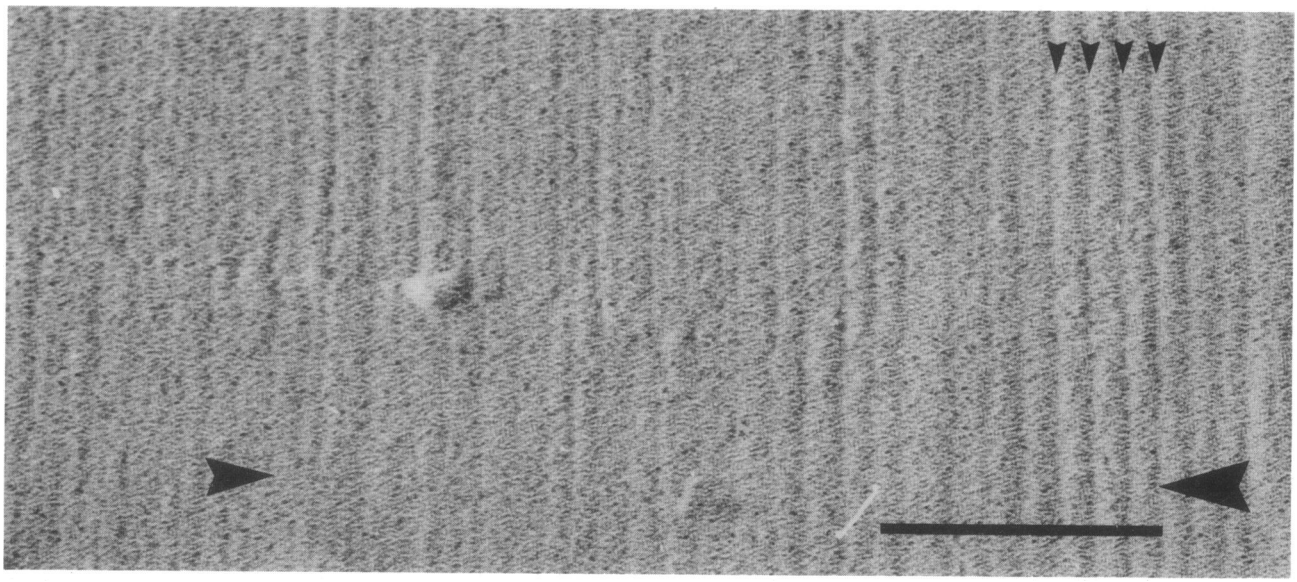

FIG. 5. Electron micrograph of sheath shadowed with platinum at an angle of 45°. Note the wave structure of the sheath's surface (small arrowheads) which highlights the hoops which make up the sheath. The midsize arrowhead indicates the longitudinal orientation of the sheath. The shadow direction is indicated by the large arrowhead. Bar, 0.2 μm.

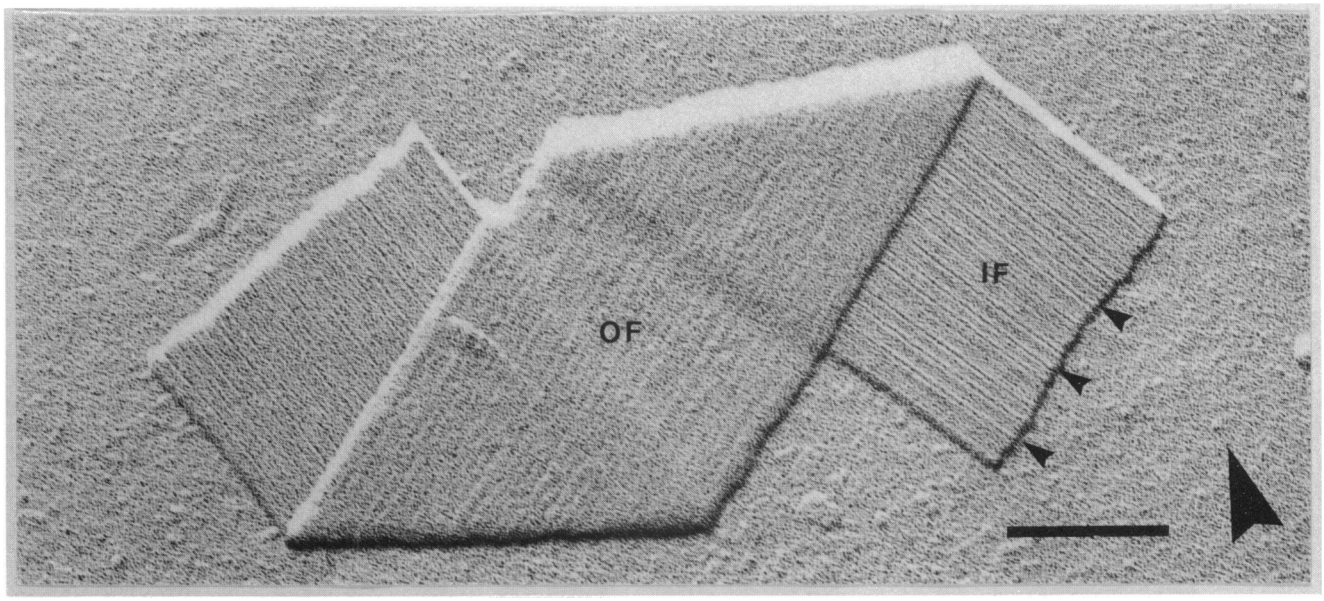

FIG. 6. Electron micrograph of French press-sheared sheath platinum shadowed at an angle of 45°. The direction of the shadow is indicated by the large arrowhead. The inner face (IF) of the sheath possesses ridges, not present on the outer face (OF), which correspond to the hoop boundaries. The ridges are emphasized by adjacent "clear" zones (small arrowheads) which correspond to the shadowed regions on the preparation. Bar, 0.2 μm.

conformational antibody probes, presented in Fig. 7, distinguishes between antibody probes with reactivity toward high-molecular-mass (~40-kDa) SDS/β-ME/EDTA-solubilized sheath proteins (conformational) and those with reactivity toward the complete range of SDS/β-ME/EDTA-solubilized proteins (10 to 40 kDa; chemical).

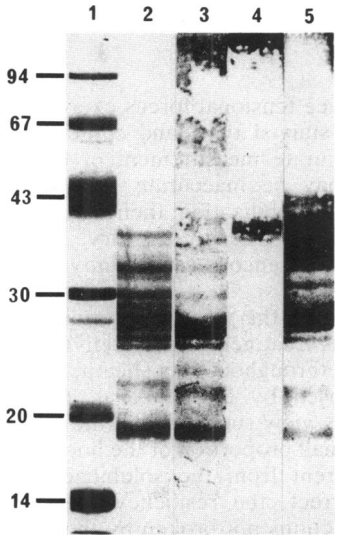

FIG. 7. Western immunoblot of SDS/β-ME/EDTA-solubilized sheath components (2 h at 100°C). Lane 1 contains protein standards, and lane 2 contains the sheath components stained with Coomassie brilliant blue R250. Lane 3 is probed with MAb 25.1, lane 4 is probed with MAb 26.1, and lane 5 is probed with Pαsera raised against the 18-kDa sheath polypeptide (refer to Fig. 1, lane 5). MAb 25.1 and rabbit anti-18-kDa Pαsera appear to possess broad chemical specificity, while MAb 26.1 may possess conformational specificity towards a more intact form of the polypeptide. Molecular masses are in kilodaltons.

DISCUSSION

The resiliency of the sheath has facilitated its purification. Few other biostructures (e.g., *Methanosaeta concilii* sheath) (19, 20) are resistant to consecutive treatments with 0.1 M NaOH and 1% (wt/vol) SDS at 90°C. Although Sprott et al. (24) suggested that the SDS treatment used in sheath purification removed sheath components, it does not seem likely that these are essential components of the sheath structure. SDS-PAGE examination of proteins extracted from a crude sheath preparation (during purification) revealed no distinct polypeptides related to the sheath (data not shown). This treatment with SDS should remove noncovalently bound material, perhaps components such as adhering membrane, cell wall, or sheath polypeptides which have undergone translocation but not chemical integration. Removal of nonintegrated polypeptides was considered essential for the subsequent study of the sheath.

Chemical characterization of *M. hungatei* GP1 sheath was based on the SDS/β-ME/EDTA dissolution treatment and represents a qualitative improvement in solubilization over the L-Arg treatment (Fig. 1, lane 2) and a quantitative improvement in solubilization over the SDS/β-ME/CHES treatment. Both the SDS/β-ME/EDTA and the L-Arg treatments solubilized 74% of the sheath's mass; however, the L-Arg treatment broke up the sheath indiscriminately. The SDS/β-ME/EDTA treatment solubilized polypeptides with molecular masses ranging between 10 and 40 kDa (Fig. 1, lane 4). These soluble fractions may represent a more labile portion of the sheath in contrast to the remaining insoluble material (26%). This fraction, which did not denature, may be chemically different from the soluble sheath components and may consist of entirely novel, insoluble sheath components. The SDS/β-ME/EDTA treatment differed from the

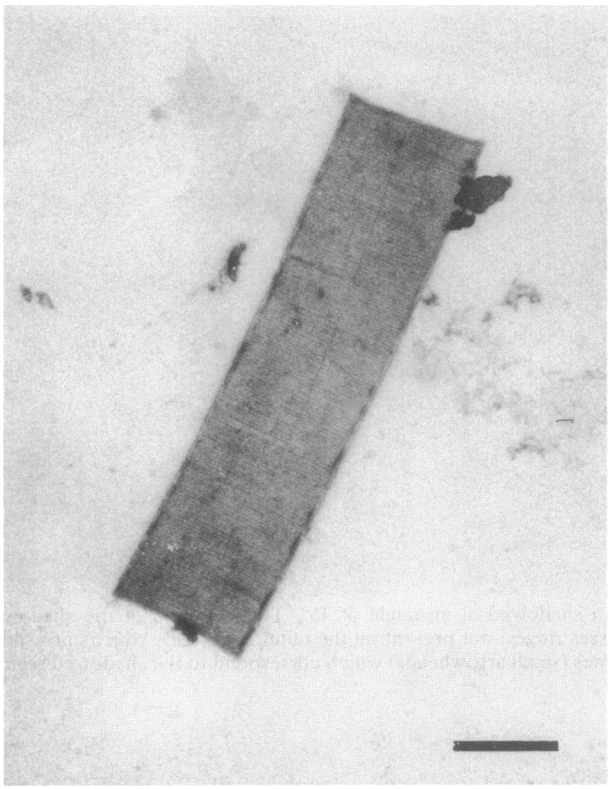

FIG. 8. Negative stain of sheath probed with protein A-colloidal gold alone (as a control and not in conjunction with antibody). The lack of labeling with colloidal gold evident in this micrograph provides confidence in our method of (antibody-mediated protein A-colloidal gold) surface localization of the SDS/β-ME/EDTA-solubilized proteins. Bar, 0.5 μm.

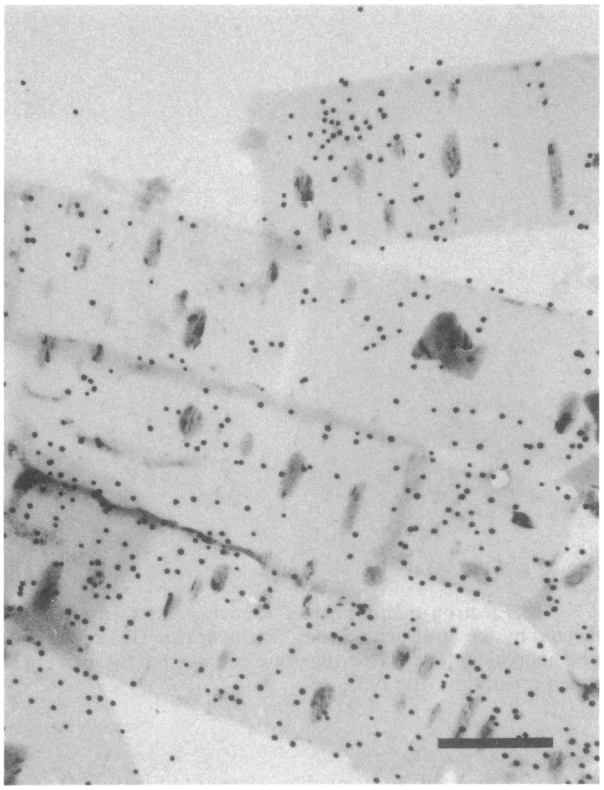

FIG. 9. Unstained whole mount of *M. hungatei* GP1 sheath labeled with MAb 26.1 (a possible conformational specific immunological probe towards the SDS/β-ME/EDTA-solubilized proteins) and protein A-colloidal gold. The colloidal gold was observed at random sites along the sheath tube. This micrograph is representative of the labeling patterns observed for MAb 25.1 and the rabbit anti-18-kDa Pαsera–protein A-colloidal gold labeling experiments. Bar, 0.5 μm.

SDS/β-ME/CHES treatment in three ways. First, this reaction proceeded at pH 6.8, which is thought to be less deleterious than the pH 9.0 of the CHES buffer system. Second, the EDTA reaction employed 5% β-ME instead of 2%, which had previously been recommended for sheath solubilization (23). Third, the incorporation of 20 mM EDTA into the reaction provided an efficient multivalent metallo-ion chelator. Patel et al. (20) suggested that Ca^{2+} may be involved with the salt bridging of constituents within the sheath.

The resiliency of the sheath is remarkable. By using EM as an accurate monitoring technique, treatments with L-Arg (pH 12.6), SDS/β-ME/CHES, or SDS/β-ME/EDTA were not completely successful for the total solubilization of the sheath structure. Hoops which possessed 2.8-nm striations on their external surface were recovered by all dissolution techniques (Fig. 2 and 3). Also, the hoops produced by these dissolution techniques had the same thickness as those in intact sheath (i.e., 10 nm). Sprott et al. (23) described hoops as potential sheath building blocks. Our new observations suggest that there might be two types of hoops, those sensitive to solubilization and those resistant to solubilization, which are structurally identical at the TEM level. Our previous work (23, 26) and that of Shaw et al. (21) has shown that the width of hoops is variable but their circumference and thickness are constant. So far, we have not been able to correlate hoop width with degree of resiliency. Although it is easy to determine the presence or absence of hoops by TEM, the surface tensional forces exerted on them as they are negatively stained twist and contort them to such an extent that accurate measurement of the particle lines is difficult and may be inaccurate. If hoops vary in their susceptibility to solubilization, then the resistant hoops must possess a subtly different chemistry. This assumption is based on the homogeneous crystallinity of the sheath structure by TEM.

An alternative to the view that certain hoops are solubilized is that this treatment has selectively solubilized components found throughout the sheath, similar to the glue peptides proposed by Sprott et al. (23) but of greater magnitude. This view suggests that the resilient hoops represent only a small proportion of the hoops and that they are somehow different from the solubilized material. If this concept is correct, the resiliency may involve different chemical interactions not broken by these dissolution techniques; perhaps it relates to a different group of proteins which resist these dissolution conditions.

With regard to the sheath's stability, it is important to note that, except by using extremes in pH or performic acid, complete solubilization of the sheath has not been possible (4). Its resistance to all chemical perturbants other than covalent bond breakers (4) emphasizes the likelihood of covalent bonding in the sheath. Covalent linkage is not usually invoked for subunit-subunit or subunit-wall bonding

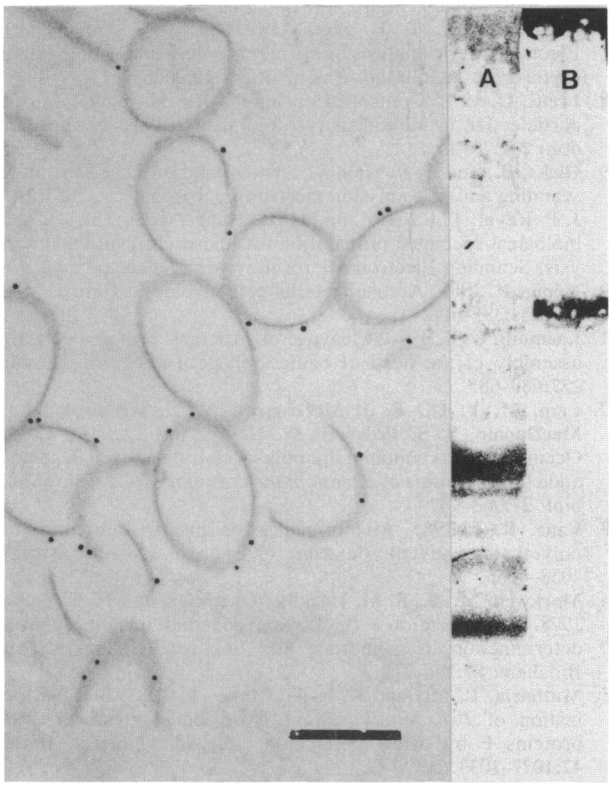

FIG. 10. Thin section of sheath labeled with MAb 26.1 and protein A-colloidal gold. Colloidal gold was observed exclusively along the outer surface of the sheath. Both chemical (MAb 25.1) (A) and conformational (MAb 26.1) (B) epitopes were localized to the outer surface. Bar, 0.5 μm.

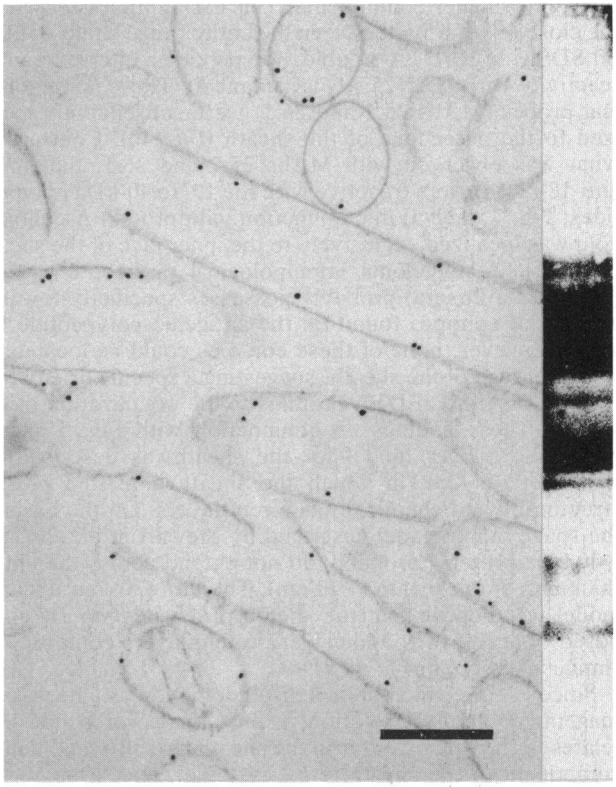

FIG. 11. Thin section of sheath labeled with rabbit anti-18-kDa Pαsera and protein A-colloidal gold. Contrary to what was observed with MAb 25.1, the rabbit anti-18-kDa Pαsera localized the colloidal gold predominantly along the inner surface of the sheath. This observation suggests that the conformational specific region of the SDS/β-ME/EDTA-solubilized proteins (MAb 26.1) may be restricted to the outer surface of the sheath (Fig. 10). Bar, 0.5 μm.

systems in most other bacterial S layers, although Beveridge et al. (4) and Sprott et al. (23) previously alluded to this possibility for the system presently discussed. Since the S layers of *Thermoproteus tenax* and *Thermofilum pendens* also resist detergent treatment (10), it is assumed they also rely on covalent bonding. If there is covalent bonding, *M. hungatei* sheath must have the capacity for covalent self-polymerization or must be under some form of enzymatic control. Presumably, there must also be stringent control over filament division (which requires a splitting of the sheath [2]) beyond mechanical (shear) breakage of the sheath at the cell spacer, since Patel et al. (17) demonstrated that *M. hungatei* filaments which measured hundreds of micrometers in length could be grown and maintained by increasing the phosphate concentration (from 3.0 to 45.0 mM) in the culture medium. How, then, are portions of the sheath which appear to be structurally homogeneous recognized for processing during the growth of the organism? The occurrence of resilient hoops suggests a possible biochemical marker beyond the resolution of EM and possibly masked within the crystalline lattice. It is possible that sheath division sites (weak zones) are incorporated in vivo. If so, these regions would be the most sensitive to fracture during sheath purification and would correspond to the ends of the purified sheath tubes.

The distinct topographical character of the inner and outer faces of the sheath was initially revealed by examination of sheared and platinum-shadowed material. In the micrographs shown in Fig. 5 and 6, the 2.8-nm periodicity in the outer face described by Beveridge et al. (4) was not evident. This confirms that the 2.8-nm repeat on the outer face of the sheath occurs in a relatively flat two-dimensional lattice (4, 21, 26) which is easily masked by the platinum shadow. Ridges ~2.0 nm in height were observed above the plane of the inner face of the sheath (Fig. 6). These ridges on the inner face could represent regions of growth within the sheath; as sheath protomers are inserted in a circumferential manner at the inner face, the added mass would bulge these regions into ridges. This concept requires that the hoops grow from their edges and increase in width. The role of adjacent ridges in linking hoops together is inferred by their physical position along the edges of the hoops. Their (potential) role in sheath growth has not been studied further.

In the molecular space-filling model by Sprott et al. (23), the 2.8-nm subunit (representing one-half of the 2.8- by 5.7-nm dimer [26]) corresponded to a 24-kDa polypeptide. They described the sheath as a protein bilayer, with an outer layer composed of 24-kDa polypeptides (which do not extend across the thickness of the sheath) and an inner layer composed of generally amorphous, high-molecular-weight material. In our present study, the SDS/β-ME/EDTA-solubilized polypeptides (10 to 40 kDa) have been located at both the inner and the outer faces of the sheath. It is possible that the lower range of these polypeptides (<40 kDa) represents degradation products of the ~40-kDa polypeptides (probably the result of extensive boiling), since immunological reactivity of MAb 26.1 towards these proteins was not observed (Fig. 7, lane 4). The reactive epitope of MAb 26.1 must be inactivated during the degradation of the ~40-kDa polypep-

tides into smaller components. This assumption is based on the close relationship between the entire range (10 to 40 kDa) of SDS/β-ME/EDTA-soluble polypeptides inferred by its reactivity with MAb 25.1 (Fig. 7, lane 3). These immunological probes (MAbs 25.1 and 26.1) were subsequently localized to the outer face of the sheath (Fig. 10). Contrary to what was observed with MAbs 25.1 and 26.1, the rabbit anti-18-kDa Pαsera (reactive with the 10- to 40-kDa polypeptides; Fig. 7, lane 5) in conjunction with protein A-colloidal gold was localized exclusively to the inner face of the sheath (Fig. 11). A polyclonal immunological probe (i.e., rabbit anti-18-kDa Pαsera) probably possesses specificity towards a range of epitopes found on the antigenic polypeptide (18 kDa); however, none of these epitopes could be located on the outer face of the sheath, suggesting a specific orientation of the SDS/β-ME/EDTA proteins in the organization of the sheath. These findings, in conjunction with Fig. 5 and 6, refute the bilayer model for the sheath, as described by Sprott et al. (23), in which the sheath consisted of two structurally and chemically different layers. On the basis of the space-filling model described by Stewart et al. (26), the ~40-kDa proteins probably do not extend across the entire thickness of the sheath (~10 nm). Therefore, in our updated model we propose that the sheath of *M. hungatei* is composed of at least two molecular protein layers composed of similar polypeptides (~40 kDa).

Since β-ME, which breaks disulfide bonds, is a necessary reagent for good dissolution, a final unanswered question relates to the role of sulfur in the sheath. Is sulfur an integral component of the sheath (e.g., cysteine), and, if so, is the sulfur related to the polypeptides solubilized by the SDS/β-ME/EDTA treatment? If these solubilized polypeptides are sulfur-containing proteins and if they are involved in intersubunit disulfide linkages, their presence at strategic locations would then help explain the resiliency of the sheath.

ACKNOWLEDGMENTS

G.S. was supported by a Natural Sciences and Engineering Research Council of Canada Graduate Student Fellowship during this study. The actual research was supported by an operating grant from the Medical Research Council of Canada to T.J.B.

The assistance of G. D. Sprott, Division of Biological Sciences, National Research Council of Canada, for advice and for growing large quantities of *M. hungatei* is greatly appreciated.

REFERENCES

1. **Bendayan, M.** 1982. Double immunocytochemical labelling applying the protein A-gold technique. J. Histochem. Cytochem. **30**:81–85.
2. **Beveridge, T. J., B. J. Harris, and G. D. Sprott.** 1987. Septation and filament splitting in *Methanospirillum hungatei*. Can. J. Microbiol. **33**:725–732.
3. **Beveridge, T. J., G. Southam, M. H. Jericho, and B. L. Blackford.** 1990. High-resolution topography of the S-layer sheath of the archaebacterium *Methanospirillum hungatei* provided by scanning tunneling microscopy. J. Bacteriol. **172**:6589–6595.
4. **Beveridge, T. J., M. Stewart, R. J. Doyle, and G. D. Sprott.** 1985. Unusual stability of the *Methanospirillum hungatei* sheath. J. Bacteriol. **162**:728–737.
5. **Burnette, W. N.** 1981. "Western blotting": electrophoretic transfer of proteins from sodium dodecyl sulfate-polyacrylamide gels to unmodified nitrocellulose and radiographic detection with antibody and radioiodinated protein A. Anal. Biochem. **112**:195–203.
6. **Conway de Macario, E., H. König, and A. J. L. Macario.** 1986. Antigenic determinants distinctive of *Methanospirillum hungatei* and *Methanogenium cariaci* identified by monoclonal antibodies. Arch. Microbiol. **144**:20–24.
7. **Fairbanks, G., T. L. Steck, and D. F. H. Wallach.** 1971. Electrophoretic analysis of the major polypeptides of the human erythrocyte membrane. Biochemistry **10**:2606–2617.
8. **Frens, G.** 1973. Controlled nucleation for the regulation of the particle size in monodisperse gold suspensions. Nature (London) **241**:20–22.
9. **Hicks, D., and R. S. Molday.** 1984. Analysis of cell labelling for scanning and transmission electron microscopy, p. 203–219. *In* J. P. Revel, T. Barnard, and G. H. Haggis (ed.), The science of biological specimen preparation for microscopy and microanalysis. Scanning Electron Microscopy Inc., Chicago.
10. **König, H.** 1988. Archaebacterial cell envelopes. Can. J. Microbiol. **34**:395–406.
11. **Laemmli, U. K.** 1970. Cleavage of structural proteins during the assembly of the head of bacteriophage T4. Nature (London) **227**:680–685.
12. **Lam, M. Y. C., E. J. McGroarty, A. M. Kropinski, L. A. MacDonald, S. S. Pedersen, N. Høiby, and J. S. Lam.** 1989. Occurrence of a common lipopolysaccharide antigen in standard and clinical strains of *Pseudomonas aeruginosa*. J. Clin. Microbiol. **27**:962–967.
13. **Lane, R. I.** 1985. Membrane fusion due to dehydration by polyethylene glycol, dextran, or sucrose. Biochemistry **24**: 4058–4066.
14. **Markwell, M. A., S. M. Haas, L. L. Breter, and N. E. Tolbert.** 1978. A modification of the Lowry procedure to simplify protein determination in membrane and lipoprotein samples. Anal. Biochem. **87**:206–210.
15. **Mutharia, L. M., and R. E. W. Hancock.** 1983. Surface localization of *Pseudomonas aeruginosa* outer membrane porin proteins F by using monoclonal antibodies. Infect. Immun. **42**:1027–1033.
16. **Oi, V. T., and L. A. Herzenberg.** 1979. Immunoglobulin-producing hybrid cell lines, p. 351–372. *In* B. B. Mishell and S. M. Shiigi (ed.), Selected methods in cellular immunology. W. H. Freeman and Co., San Francisco.
17. **Patel, G. B., L. A. Roth, and G. D. Sprott.** 1979. Factors influencing filament length of *Methanospirillum hungatii*. J. Gen. Microbiol. **112**:411–415.
18. **Patel, G. B., L. A. Roth, L. van den Berg, and D. S. Clark.** 1976. Characterization of a strain of *Methanospirillum hungatii*. Can. J. Microbiol. **22**:1404–1410.
19. **Patel, G. B., and G. D. Sprott.** 1990. *Methanosaeta concilii* gen. nov., sp. nov. ("*Methanothrix concilii*") and *Methanosaeta thermoacetophila* nom. rev., comb. nov. Int. J. Syst. Bacteriol. **40**:79–82.
20. **Patel, G. B., G. D. Sprott, R. W. Humphrey, and T. J. Beveridge.** 1986. Comparative analysis of the sheath structures of *Methanothrix concilii* GP6 and *Methanospirillum hungatei* strains GP1 and JF1. Can. J. Microbiol. **32**:623–631.
21. **Shaw, P. J., G. J. Hills, J. A. Henwood, J. E. Harris, and D. B. Archer.** 1985. Three-dimensional architecture of the cell sheath and septa of *Methanospirillum hungatei*. J. Bacteriol. **161**:750–757.
22. **Sleytr, U. B., and P. Messner.** 1988. Crystalline surface layers in prokaryotes. J. Bacteriol. **170**:2891–2897.
23. **Sprott, G. D., T. J. Beveridge, G. B. Patel, and G. Ferrante.** 1986. Sheath disassembly in *Methanospirillum hungatei* strain GP1. Can. J. Microbiol. **32**:847–854.
24. **Sprott, G. D., J. R. Colvin, and R. C. McKellar.** 1979. Spheroplasts of *Methanospirillum hungatii* formed upon treatment with dithiothreitol. Can. J. Microbiol. **25**:730–738.
25. **Sprott, G. D., and R. C. McKellar.** 1980. Composition and properties of the cell wall of *Methanospirillum hungatei*. Can. J. Microbiol. **26**:115–120.
26. **Stewart, M., T. J. Beveridge, and G. D. Sprott.** 1985. Crystalline order to high resolution in the sheath of *Methanospirillum hungatei*: a cross-beta structure. J. Mol. Biol. **183**:509–515.
27. **Towbin, M., T. Staehelin, and J. Gordon.** 1979. Electrophoretic transfer of proteins from polyacrylamide gels to nitrocellulose sheets: procedure and some applications. Proc. Natl. Acad. Sci. USA **76**:4350–4354.